

Photochemistry of an Ozone Molecular Complex with Iodine Monochloride in Cryogenic Matrices. The Infrared Spectra of Iodosyl Chloride (OICl) and Iodyl Chloride (O₂ICl)

Michael Hawkins,^{†,‡} Lester Andrews,*[†] Anthony J. Downs,[‡] and David J. Drury*^{‡,§}

Contribution from the Department of Chemistry, University of Virginia, Charlottesville, Virginia 22901, and the Department of Inorganic Chemistry, University of Oxford, South Parks Road, Oxford OX1 3QR, England. Received September 6, 1983

Abstract: Codeposition of ozone and iodine monochloride in argon, krypton, or nitrogen matrices leads to the formation of a 1:1 molecular complex O₃·ICl. Extremely photosensitive to radiation between 470 and 750 nm, the complex photodissociates to iodosyl chloride, OICl. Further, decomposition of OICl to yield oxygen atoms is the probable origin of a second product iodyl chloride, O₂ICl. Normal coordinate calculations reveal the -IO₂ moiety to be vibrationally independent of the chlorine atom, a result interpreted as arising from the large mass of the central iodine atom and an I-Cl bond with a high degree of ionic character. Both iodosyl and iodyl chloride decompose when irradiated with ultraviolet light between 240 and 320 nm.

Molecular π complexes between aromatic systems and ozone are known to absorb visible light between 380 and 560 nm.¹ Visible absorption occurs at longer wavelength as the ionization potential of the π system is reduced, suggesting charge transfer from the aromatic molecule to ozone during excitation. The role of such complexes in the ozonation of aromatic systems remains unclear while the very existence of molecular ozone complexes with aliphatic π systems is uncertain.²⁻⁴ There is some evidence that ozone forms a molecular complex with certain inorganic substrates, for example, chlorine monofluoride⁵ and phosphorus and arsenic trifluorides.⁶ Well-defined perturbations in the infrared spectrum of either ozone or the substrate when co-condensed in an argon matrix at 15-20 K suggested a specific molecular interaction. Although no ultraviolet/visible absorption spectra were recorded for these systems, both groups of workers noted photochemical behavior for the perturbed species different from that of isolated, monomeric ozone.

These findings have prompted a more rigorous search for molecules which modify the photochemical behavior of ozone when the two reagents are co-condensed in cryogenic matrices. In the case of monovalent compounds of iodine, ultraviolet or visible irradiation of the matrix might also provide a method of preparing and characterizing hitherto unknown monomeric iodosyl and iodyl molecular species. Although several aromatic compounds of molecular formula ArIO and ArIO₂ (Ar = aryl) are well characterized,^{7,8} few corresponding aliphatic or inorganic compounds have been prepared.⁹⁻¹⁴ Inorganic iodosyl compounds appear to be polymeric in the solid state, as evidenced by the crystal structure of the sulfate, (IO)₂SO₄,¹⁵ and it is only for the (trifluoromethyl)sulfonate, IOSO₂CF₃, that the vibrational spectrum provides evidence of a discrete IO unit.⁹ Although vibrational spectra of three iodyl compounds, the fluorosulfonate,¹² the (trifluoromethyl)sulfonate,⁹ and the difluorodioxo phosphate (IO₂PO₂F₂),¹³ suggest solid-state structures involving discrete IO₂ units, there are no reports to date of simple mononuclear species of the type X-I=O or X-IO₂ where the univalent substituent X is bound covalently to iodine. Here follows an account of a matrix study where visible photolysis of a molecular ozone-iodine monochloride complex leads to formation of iodosyl and iodyl chloride.

Experimental Section

Apparatus. The cryogenic refrigeration system and vacuum vessel have been described in detail elsewhere.¹⁶ Infrared spectra were recorded

on a Beckman IR-12 spectrophotometer over the range 200-2000 cm⁻¹. Regions of interest were examined by using expanded wavenumber scales allowing measurement of band positions to better than ± 1 cm⁻¹. Ultraviolet/visible absorption spectra were recorded on a Cary 17 spectrophotometer interfaced with an Apple II computer for purposes of spectral data collection and analysis. Between one and ten data points per nanometer were collected, and the signal at each point was averaged over two to ten measurements. The temperature of the CsI cold window in the range 14-25 K was determined by a H₂ vapor-pressure gauge attached to the second stage of the refrigerator cold tip and was varied by adjusting the voltage applied to three heater buttons (Minco Products Inc., Minneapolis, MN) mounted on the copper window support. Samples were photolyzed for periods between 30 sec and 65 min by a BH-6 high-pressure mercury arc (1000 W, Illumination Industries Inc.). A 10-cm water filter reduced the infrared radiation incident upon the matrix during photolysis while a germanium filter inserted in the beam of the infrared spectrophotometer prevented sample photolysis by visible radiation from the Nernst glower. Several optical filters were used to transmit selected regions of the Hg arc emission for photolysis. A saturated aqueous NiSO₄/CoSO₄ solution and two band-pass filters gave access to the regions 235-335, 240-420, and 340-600 nm, respectively, while Pyrex and a cutoff filter were used to remove radiation of wavelength shorter than 290 and 470 nm, respectively.

Chemicals. The argon and nitrogen (Air Products) and krypton (Airco Industrial Gases) were used as supplied without further purification. Ozone was generated by a static electric discharge (Tesla coil) of oxygen in a Pyrex tube immersed in liquid nitrogen.¹⁷ Residual O₂ was removed by pumping at 77 K with an oil diffusion pump. Normal isotopic oxygen (Burdett, U.S.P.) and 50.3 and 98.0% ¹⁸O-enriched oxygen gas (Yeda, Israel) were used directly. Iodine monochloride (Aldrich) was stored

(1) Bailey, P. S. "Organic Chemistry"; Wasserman, H. H., Ed.; Academic Press: New York, 1982; Vol. 39 Chapter 11.

(2) Hull, L. A.; Hisatsune, I. C.; Heicklen, J. J. *Am. Chem. Soc.* **1972**, *94*, 4856.

(3) Alcock, W. G.; Mile, B. J. *Chem. Soc., Chem. Commun.* **1976**, 5.

(4) Nelander, B.; Nord, L. *J. Am. Chem. Soc.* **1979**, *101*, 3769.

(5) Andrews, L.; Chi, F. K.; Arkell, A. J. *Am. Chem. Soc.* **1974**, *96*, 1997.

(6) Downs, A. J.; Gaskill, G. P.; Saville, S. B. *Inorg. Chem.* **1982**, *21*, 3385. Gaskill, G. P. D. Phil. Thesis, University of Oxford, 1978.

(7) Banks, D. F. *Chem. Rev.* **1966**, *66*, 243.

(8) Downs, A. J.; Adams, C. J. "The Chemistry of Chlorine, Bromine, Iodine and Astatine"; Pergamon: Oxford, 1975.

(9) Dalziel, J. R.; Carter, H. A.; Aubke, F. *Inorg. Chem.* **1976**, *15*, 1247.

(10) Ellestad, O. H.; Woldbaek, T.; Kjekshus, A.; Klæboe, P.; Selte, K. *Acta Chem. Scand., Ser. A* **1981**, *A35*, 155.

(11) Schmeisser, M.; Naumann, D.; Renk, E. Z. *Anorg. Allg. Chem.* **1980**, *470*, 84.

(12) Carter, H. A.; Aubke, F. *Inorg. Chem.* **1971**, *10*, 2296.

(13) Addou, A.; Vast, P. J. *Fluorine Chem.* **1980**, *16*, 89.

(14) Naumann, D.; Deneken, L.; Renk, E. J. *Fluorine Chem.* **1975**, *5*, 509.

(15) Furuseth, S.; Selte, K.; Hope, H.; Kjekshus, A.; Klewe, B. *Acta Chem. Scand., Ser. A* **1974**, *A28*, 71.

(16) Andrews, L. *J. Chem. Phys.* **1968**, *48*, 972; **1971**, *54*, 4935.

(17) Andrews, L.; Spiker, R. C., Jr. *J. Phys. Chem.* **1972**, *76*, 3208.

[†] University of Virginia.

[‡] Present address: Sevenoaks School, Sevenoaks, Kent TN13 1HU, U.K.

[§] University of Oxford.

[§] Present address: Research and Development Department, BP Chemicals Limited, Salt End, Hull HU12 8DS, U.K.

Table I. The Frequencies (in cm^{-1}) of Absorptions Associated with ICl and the Complex $\text{O}_3\cdot\text{ICl}$ in the Infrared Spectrum of Matrices Containing Ozone and Iodine Monochloride

argon			krypton	nitrogen	assignment
$^{16}\text{O}_3$	$^{16,18}\text{O}_3$	$^{18}\text{O}_3$	$^{16}\text{O}_3$	$^{16}\text{O}_3$	
1110.8			1107.0		$\nu_{\text{sym}}(\text{O}_3), \text{O}_3\cdot\text{ICl}$
	1105.6		1104.2	1110.0 ^a	
	1180.8				
	1076.5	1048.2			$\nu_{\text{asym}}(\text{O}_3), \text{O}_3\cdot\text{ICl}$
1019.5			1016.5	1023.0	
	997.2		1011.3		
	986.5 ^b				$\delta_{000}(\text{O}_3), \text{O}_3\cdot\text{ICl}$
	967.3	964.0			
704.3 ^a	963.7		702.3 ^a	711.4	
		667.5 (sh)			$\nu_{\text{ICl}}, \text{I}^{35}\text{Cl}$
376.2	375.8	375.9	375.1	376.5	
372.1	372.5	372.3	375.1 ^a	376.5 ^a	$\nu_{\text{ICl}}, \text{O}_3\cdot\text{I}^{35}\text{Cl}$
368.1	368.2	368.2	367.2	368.4	$\nu_{\text{ICl}}, \text{I}^{37}\text{Cl}$
364.1	364.6 (sh) ^d	364.2 (sh)	367.2 ^a	368.4 ^a	$\nu_{\text{ICl}}, \text{O}_3\cdot\text{I}^{37}\text{Cl}$
357.8	358.0	358.1	359.6 (sh)	355.2 ^c	$(\text{ICl})_x$
350.5	350.3 (sh)	350.1 (sh)	355.0 (sh)	347.3 ^c	$(\text{ICl})_x$

^aObscured by a parent absorption. The wavenumber quoted is that of either uncomplexed ozone or iodine monochloride, and the assignment is made on the basis of a decrease in absorbance on irradiation of the matrix at $\lambda > 470$ nm. ^bNo specific band is observed because of coincidence with uncomplexed $^{16}\text{O}_3$ - $^{18}\text{O}_3$ isotopomers. However, the optical density decreased by 42% at this wavenumber on irradiation of the matrix at $\lambda > 470$ nm. ^cIodine monochloride aggregate bands are very weak in a nitrogen matrix. ^dsh denotes shoulder absorption.

under vacuum in a Pyrex ampule fitted with a greaseless, Teflon tap and wrapped with aluminum foil to exclude light. The sample was degassed by freeze-thawing and pumping at 77 K and, immediately prior to use, any hydrogen chloride, hydrogen iodide, or chlorine were removed by pumping at -45 °C.

Procedure. Ozone was diluted with matrix gas to a matrix ratio (M/R) between 100/1 and 800/1 and deposited at 14 K at an average rate of 5 mmol/h for 4 h. Iodine monochloride was co-condensed with the diluted ozone by pumping it directly from its storage ampule at -45 °C; this technique reduced dissociation to iodine and chlorine and hydrolysis to hydrogen chloride. The concentration of iodine monochloride in the sample was not known, but the degree of isolation of ICl monomer could be monitored by the infrared spectrum and controlled by using the ampule tap to regulate the flow of ICl vapor. Infrared and UV/vis experiments were conducted in a similar fashion in the interests of consistency except that the former required longer deposition periods.

Results

Ultraviolet/Visible and Infrared Spectra after Matrix Deposition.

The UV/vis absorption spectrum of an argon matrix containing ozone (M/R = 100/1) between 300 and 800 nm was featureless except for the long-wavelength tail of the intense Hartley band of ozone which extended to 315 nm. The deposition of argon plus ICl gave rise to a weak broad absorption between 300 and 560 nm with a maximum at 440 nm. In separate experiments, ICl codeposited with ozone diluted with either argon or nitrogen (M/R = 100/1) yielded broad bands between 345 and 625 (Ar) and 350 and 600 nm (N_2) with well-defined maxima at 460 and 440 nm, respectively.

Codeposition of ICl with ozone diluted with argon (M/R = 100/1) gave the infrared spectrum of Figure 1a. In addition to bands characteristic of ozone¹⁷ at 1104.9, 1040.5, 1033.6, and 704.3 cm^{-1} and iodine monochloride at 376.2, 368.1, 357.8, and 350.5 cm^{-1} (Figure 2a, Table I), absorptions were observed at 1110.8 and 1019.5 cm^{-1} (Figure 1a) and 372.1 and 364.1 cm^{-1} (Figure 2b). These features were not present in the infrared spectrum of argon matrices containing O_3 or ICl alone. The absorptions at 1110.8 and 1019.5 cm^{-1} exhibit a 1/9 relative intensity while the intensities of the symmetric and antisymmetric stretches of ozone are in the ratio 1/70.¹⁷ Codeposition of 98% ^{18}O -enriched ozone with ICl gave rise to absorptions, in addition to those characteristic of the parent molecules, at 1048.2, 964.0, 372.3, and 364.2 cm^{-1} which exhibited shifts of -62.6 , -55.5 , 0.2 ,

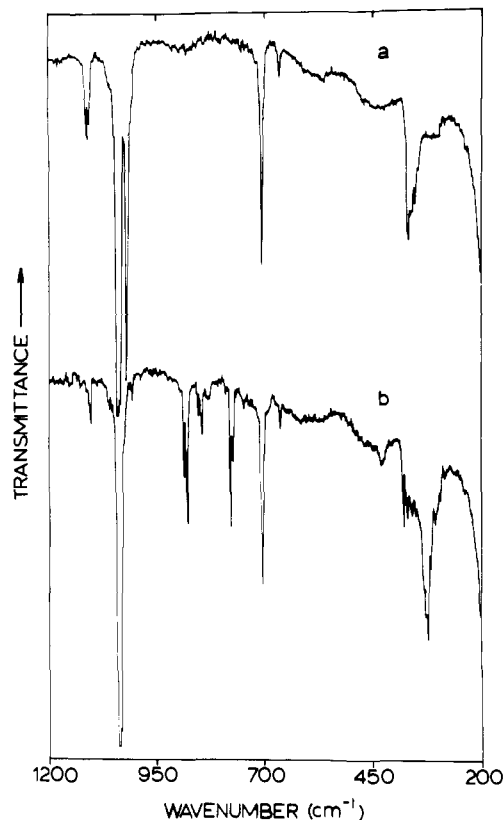


Figure 1. The infrared spectrum between 200 and 1200 cm^{-1} of an argon matrix containing iodine monochloride and ozone ($\text{Ar}/\text{O}_3 = 100/1$) deposited at 14 K: (a) after deposition and (b) after filtered Hg arc irradiation first with $\lambda > 590$ nm for 15 min then $\lambda > 470$ nm for 15 min.

and 0.1 cm^{-1} , respectively, with respect to their $^{16}\text{O}_3$ counterparts.

Absorptions other than those associated with ozone and iodine monochloride were also observed on their codeposition in krypton and nitrogen matrices (Table I). In krypton matrices two bands were observed at 1107.0 and 1104.2 cm^{-1} to the high-frequency side of $\nu_1(\text{O}_3)$ and two absorptions were observed to the low-

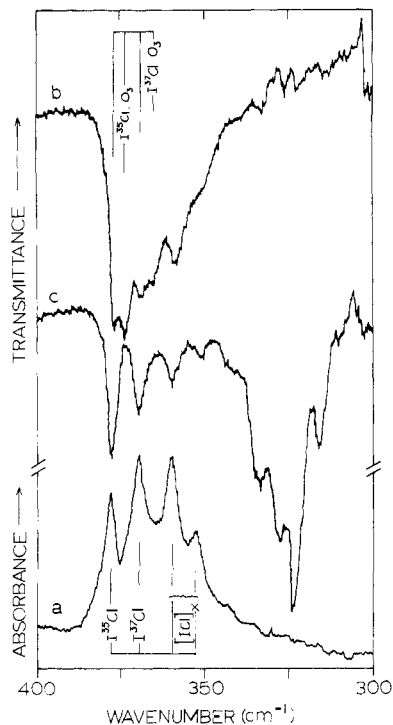


Figure 2. The infrared spectrum between 300 and 400 cm^{-1} of an argon matrix deposited at 14 K containing (a) iodine monochloride deposited for 239 min with ca. 18 mmol of Ar, (b) iodine monochloride deposited for 228 min with ca. 17.8 mmol of $\text{Ar}/^{16}\text{O}_3\text{-}^{18}\text{O}_x$ (50.35% ^{18}O enrichment, M/R = 100/1), and (c) same as in b but after being filtered with Hg arc irradiation at $340 < \lambda < 600$ nm.

frequency side of $\nu_3(\text{O}_3)$ at 1016.5 and 1011.3 cm^{-1} . No bands other than those associated with iodine monochloride or its aggregates were found between 350 and 380 cm^{-1} . The same spectral region was further simplified in nitrogen matrices: two intense bands at 376.5 and 368.4 cm^{-1} were accompanied by two very weak and broad absorptions at 355 and 347 cm^{-1} . An intense absorption was observed at 1023.0 cm^{-1} to low frequency of $\nu_3(\text{O}_3)$ but, in contrast to both argon and krypton deposits, no additional band could be resolved close to $\nu_1(\text{O}_3)$. Instead an absorption at 711.4 cm^{-1} was found near the bending mode of ozone.

Several experiments were performed to investigate how the intensity of the 1019.5- cm^{-1} absorption characteristic of iodine monochloride and ozone codeposited in an argon matrix varied with the concentration of ozone in the sample. Iodine monochloride was deposited at a constant rate throughout, and mixtures of ozone in argon with M/R between 200/1 and 800/1 were deposited at approximately constant rates between 4.2 and 4.8 mmol/h. Several measurements of the peak absorbance at 1019.5 cm^{-1} were made during a single experiment and were normalized to those corresponding to the deposition of 1 in. (25 torr) of argon/ozone mixture. A plot of the log of these normalized values against the log of the mole percent ozone in the argon/ozone mixture is illustrated in Figure 3. The plot is linear and the gradient is 1.0 ± 0.2 .

Ultraviolet/Visible Hg Arc Irradiation of Matrices Containing O_3 and ICl. Irradiation of an argon matrix containing ozone and iodine monochloride at 470–1000 nm for 11 min reduced the broad 460-nm absorption band by 30–40%. In addition another band was produced, which was full scale at wavelengths shorter than 330 nm, extended to 400 nm, and exhibited no maximum in this region. Subsequent irradiation between 290 and 400 nm for 15 min reduced this new absorption by 40% at 330 nm.

The infrared spectrum of an argon matrix formed by codeposition of iodine monochloride and an argon/ozone mixture (M/R = 100/1) exhibited all the absorptions listed in the left-hand column of Table I plus those of ozone itself. Exposure of the matrix to Nernst Glower radiation for 5 h decreased the absorptions at 1110.8 and 1019.5 cm^{-1} by ca. 60%. Several new

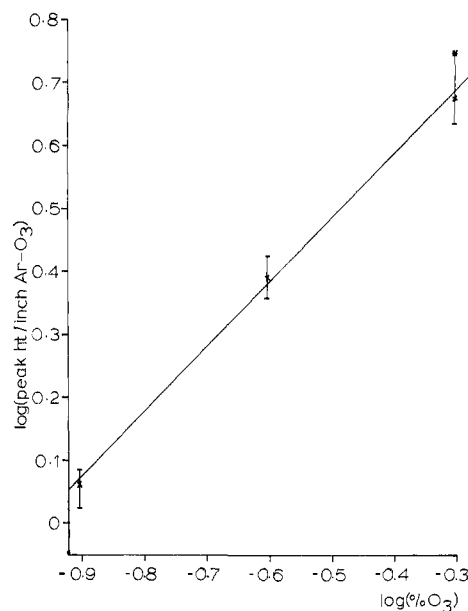


Figure 3. Relationship between the peak height (in arbitrary units) of the 1019.5- cm^{-1} absorption associated with the molecular complex $(\text{O}_3)_x(\text{ICl})_y$ and the concentration of the Ar/ O_3 matrix. Peak heights were measured directly from absorbance spectra.

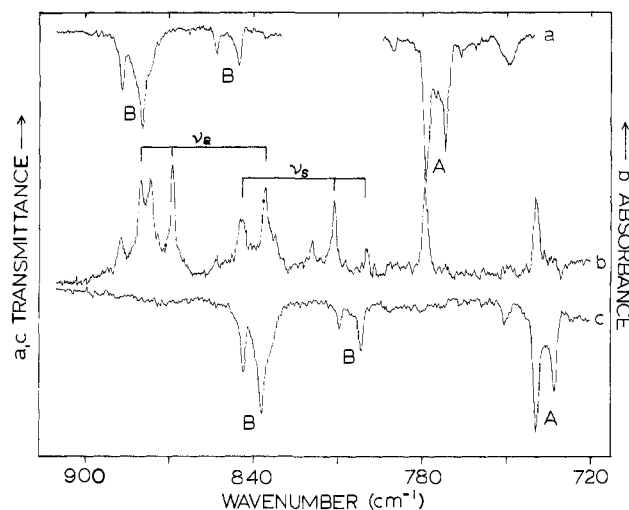


Figure 4. Infrared spectra between 720 and 910 cm^{-1} of isotopic ozone-iodine monochloride-argon samples subjected to $\lambda > 470$ nm photolysis at 14 K for 60–80-min periods: (a) $^{16}\text{O}_3$, (b) 50.3% ^{18}O -enriched, scrambled ozone, sample also subjected to 14–30–14 K warming cycle, (c) $^{18}\text{O}_3$, 95.6% ^{18}O enriched.

absorptions appeared and these are summarized in the left-hand column of Table II. The same changes were observed after 15 min of irradiation of a similar deposit with either $\lambda > 470$ nm or $340 < \lambda < 600$ nm filtered Hg arc emission. In this case the bands at 1110.8 and 1019.5 cm^{-1} were completely destroyed; a 50% reduction could be achieved with only 90-s irradiation at $\lambda > 470$ nm. Survey and high-resolution spectra of all photoproduct absorptions are shown in Figures 1b, 2c, and 4a. Exposure to Hg arc emission between 750 and 1000 nm gave a 5–10% decrease in intensity of the bands at 1110.8 and 1019.5 cm^{-1} , and their photosensitivity toward the Nernst Glower radiation was overcome by inserting a Ge-coated filter immediately after the glower. All photoproducts formed by Nernst Glower irradiation were stable to incident radiation with $\lambda > 340$ nm, except for the weak absorption shown in Figure 4 at 748.6 cm^{-1} , which decreased 33% after a further 15 min of irradiation.

Product Discrimination. The number of products were determined by sequential periods of photolysis and annealing, photolysis at different temperatures, and the additional use of

Table II. The Frequencies (in cm^{-1}) of Absorptions Observed To Grow in the Infrared Spectrum of Matrices Containing Ozone and Iodine Monochloride after Visible Irradiation^e

argon			krypton	nitrogen	product ^a	assignment
¹⁶ O ₃	^{16,18} O ₃	¹⁸ O ₃	¹⁶ O ₃	¹⁶ O ₃		
314.1	313.8	314.1	311.2	315.5	A(1)	ν_{ICl} , OI ³⁷ Cl
320.2	320.5	320.4	317.4	322.6	A(1)	ν_{ICl} , OI ³⁵ Cl
324.5	323.8	ur	ur	ur	B(1+2)	ν_{ICl} , O ₂ I ³⁷ Cl
325.6	324.9	ur	ur	ur	A(2)	ν_{ICl} , OI ³⁵ Cl
327.5	326.9	ur	331.6 ^b	ur	B(3)	ν_{ICl} , O ₂ I ³⁷ Cl
330.5	330.8	329.9	327.5	331.9	B(1+2)	ν_{ICl} , O ₂ I ³⁵ Cl
333.4	333.1	ur	339.2 ^b	339.0	B(3)	ν_{ICl} , O ₂ I ³⁵ Cl
		339.4 (br)			B(1+2)	} δIO_2 , O ₂ ICl
	410.2 (br)	406.6			B(3)	
421 (br)					B(1+2+3)	
429.9	430.4				B(1+2)	
748.6					B(3)	} unidentified
	733.3	733.3			C	
	739.9	739.8			A(2)	} ν_{IO} , OICl
772.2	772.0		775.1 ^c		A(1)	
779.1	779.1		778.2 ^c	778.2	A(2)	
791.1		751.3			A(1)	
	801.4	801.6			A(3)? ^d	} $\nu_{\text{sym}}(\text{IO}_2)$, O ₂ ICl
	812.9	809.4			B(1)	
	820.3				B(2)	
844.7	844.8		845.5	852.2	B(1)	
853.4	853.0		850.0		B(2)	} $\nu_{\text{asym}}(\text{IO}_2)$, O ₂ ICl
	836.9	837.4			B(1)	
	843.7	843.9			B(2)	
	868.6				B(1)	
	876.0				B(2)	} $\nu_{\text{asym}}(\text{IO}_2)$, O ₂ ICl
877.1 (sh)					B(3)	
879.5	879.6		879.6	879.7	B(1)	
886.5	886.5		883.5	883.7	B(2)	

^aNumbers in parentheses are used to distinguish different matrix sites. Site splitting refers to argon and krypton matrices. In nitrogen only $\nu_{\text{asym}}(\text{IO}_2)$ of O₂ICl showed a site splitting. ^bTentative assignment. ^cThe relative intensity of these bands is inverted compared with the corresponding absorptions in argon at 772.2 and 779.1 cm^{-1} . ^dTentatively assigned to a third site of OICl on the basis of the observed ¹⁸O isotopic shift. ^ebr = broad; ur = unresolved.

krypton and nitrogen matrices. An experiment was performed consisting of the following sequence of operations: (i) 15 min of irradiation at 14 K with $\lambda > 590$ nm; (ii) 15 min of irradiation at 14 K with $\lambda > 470$ nm; (iii) annealing to 28 K for 3 min followed by recooling to 14 K; (iv) annealing to 30–31 K for 30 min followed by recooling to 14 K; (v) warming to 20 K before irradiation at 20 K for 15 min with $\lambda > 470$ nm followed by recooling to 14 K; (vi) annealing to 33 K for 15 min followed by recooling to 14 K. It is apparent from the results of this treatment that there are two major products, A, and B, and a minor product, C. A and B are stable to visible light irradiation while C is not. The frequency separation between several pairs of absorptions between 750 and 900 cm^{-1} is compatible with that expected for a ³⁵Cl/³⁷Cl isotopic shift of a Cl–O stretching mode (6.4–7.7 cm^{-1}). However, while pairs of absorptions above 800 cm^{-1} (Figure 4a) exhibit incorrect relative intensities to be associated with chlorine isotopic products, the components at 772.2/779.1 cm^{-1} exhibited variable relative intensity. Furthermore pairs of absorptions at 772.2/779.1 and 844.7/853.2 cm^{-1} in argon matrices gave way to single bands at 778.2 and 852.2 cm^{-1} , respectively, in nitrogen matrices.

The set of absorptions between 310 and 335 cm^{-1} exhibited complex changes in intensity on both warming and photolysis. However, particular pairs of absorptions exhibited changes in relative intensity similar to those observed in the higher-frequency region, and in addition, each band was observed to be a doublet. The proximity of absorptions in this region did not allow an estimate to be made of the relative intensity of components of the doublets, but that of the doublet at 320.2/314.1 cm^{-1} is close to 3/1.

The component of lower intensity in each pair of absorptions above 750 cm^{-1} (Figure 4a) was substantially decreased in intensity

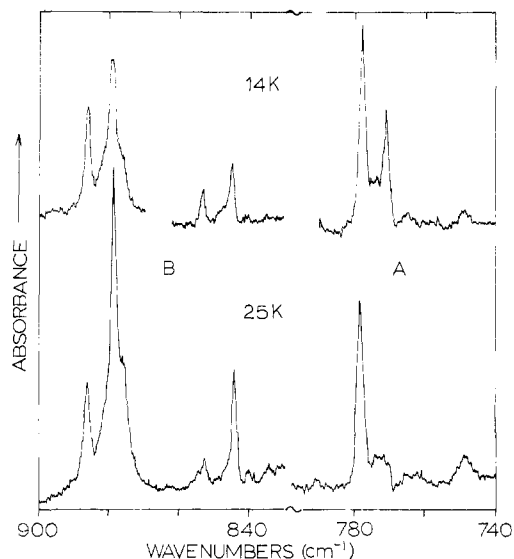


Figure 5. The influence of temperature during irradiation at $\lambda > 470$ nm on the infrared spectra and relative yields of photoproducts A (OICl) and B (O₂ICl) isolated in argon matrices containing ozone and iodine monochloride.

by warming the matrix to 28 K or above. In addition product A exhibited a much greater sensitivity to increases in temperature than product B and could be almost entirely destroyed by warming to 33 K. As a result, irradiation of the matrix with $\lambda > 470$ nm at 20–28 K rather than at 14 K leads to a single absorption at 779.1 cm^{-1} rather than a pair of bands at 779.1/772.2 cm^{-1} and,

Table III. A Comparison of the Vibrational Frequencies (in cm^{-1}) of Modes Involving IO and IO_2 Groups in Selected Iodosyl and Iodyl Compounds

mode	OICl^a	$\text{IOSO}_3\text{CF}_3^b$	O_2ICl^a	$\text{IO}_2\text{SO}_3\text{CF}_3^b$	$\text{IO}_2\text{SO}_3\text{F}^c$	TeO_2^d
$\nu(\text{IO})$	779.1 772.2	885 860				
$\nu_{\text{asym}}(\text{IO}_2)$			879.5	860	900 878	839.4
$\nu_{\text{sym}}(\text{IO}_2)$			844.7	830	865	822.6
$\delta(\text{IO}_2)$			421		428	

^aThis work. ^bInfrared, solid state, ref 9. ^cRaman, solid state, ref 12. ^dInfrared, argon matrix, ref 25.

more importantly, to a much enhanced yield of product B (Figure 5). Furthermore, krypton and nitrogen matrices at 14 K lead to relatively poor yields of product B compared with product A.

Product Characterization by ^{18}O Enrichment. Three different experiments were performed by using ozone enriched in ^{18}O . Absorptions observed before and after visible light irradiation are summarized in Tables I and II, respectively, for argon matrices containing iodine monochloride and $^{18}\text{O}_3$ (98.0% ^{18}O) or scrambled $^{16}\text{O}_{3-x}\text{O}_x$ (50.3% ^{18}O). While the photoproduct absorptions between 310 and 340 cm^{-1} exhibited no significant ^{18}O shift, those between 720 and 910 cm^{-1} were shifted by $38.9\text{--}44.0\text{ cm}^{-1}$ (columns 1 and 3, Table II, Figure 4a,c) when $^{16}\text{O}_3$ was replaced by $^{18}\text{O}_3$. Use of scrambled ozone resulted in the appearance, on visible irradiation, of all absorptions observed previously for $^{16}\text{O}_3$ and $^{18}\text{O}_3$ plus bands at 410.2, 812.9, 820.3, 868.6, and 876.0 cm^{-1} (column 2, Table II and Figure 4b). Cycles of annealing and irradiation at different temperatures distinguish two doublets between 730 and 780 cm^{-1} associated with photoproduct A and four asymmetric triplets associated with photoproduct B between 800 and 890 cm^{-1} . Absorptions associated with minor sites of photoproducts A and B decreased substantially in intensity on warming the matrix, as observed in experiments employing ozone of natural isotopic abundance; the infrared spectrum in Figure 4b was recorded after a warming cycle. Initial irradiation with $\lambda > 470\text{ nm}$ was followed by warming to 30 K and further irradiation at 22 K; comparison of Figure 4b with Figure 4, parts a and c, which were recorded after irradiation at 14 K, clearly illustrates the simplification afforded by temperature variation. Finally irradiation of an argon matrix containing iodine monochloride and the isotopes $^{16}\text{O}_3$ and $^{18}\text{O}_3$ in the ratio 1:1 resulted in an infrared spectrum identical with that in Figure 4b for scrambled $^{16}\text{O}_{3-x}\text{O}_x$.

Discussion

Discussion of the results will be presented in three parts. First the photoproducts A and B will be identified. Second the origin of absorptions present before irradiation and which cannot be attributed to the parent molecules ozone and iodine monochloride will be considered. Finally a mechanism for the formation of photoproducts A and B will be proposed.

Identification of Photoproducts A and B. Visible irradiation and temperature cycling experiments suggest that two sets of absorptions at 314.1, 320.2, and 779.1 cm^{-1} and at 325.6 and 772.2 cm^{-1} are associated with a single product, A. The thermal sensitivity of the 325.6- and 772.2-cm^{-1} bands together with their absence in nitrogen suggests two lattice sites, 1 and 2, for A isolated in solid argon. The doublets at 772.2 and 733.3 cm^{-1} (site 2) and 779.1 and 739.8 cm^{-1} (site 1) in the scrambled $^{16}\text{O}_{3-x}\text{O}_x$ experiments show that A contains a single oxygen atom. The magnitude of the ^{18}O isotopic shift is indicative of an I-O rather than a Cl-O vibration. A relative intensity of ca. 3/1 for the absorptions of 320.2 and 314.1 cm^{-1} , together with their proximity to the I-Cl fundamental of the parent iodine monochloride and the lack of an ^{18}O isotopic shift, supports assignment of these bands to $\nu(\text{I-Cl})$ of product A. The separation of 6.7 cm^{-1} is close to that expected (6.9 cm^{-1}) for an ICl diatomic at 320.2 cm^{-1} . The absence of any other absorptions associated with product A suggests that it is the triatomic OICl, iodosyl chloride. The absorption $\nu(\text{I-Cl})$ of OI^{37}Cl isolated in site 2 is obscured by the corresponding absorption for OICl in site 1, and the bending mode, expected at much lower frequency, was not observed.

Visible irradiation and temperature cycling experiments also allow discrimination between three sets of bands each denoted product B in Table III. Bands at 324.5, 330.5, 421.4, 844.7, and 879.5 cm^{-1} and 327.5, 333.4, 429.9, and 877.1 cm^{-1} are stable at the highest temperature used (33 K) while those at 853.4 and 886.5 cm^{-1} are diminished at 28 K. This thermal behavior, together with a comparison of the spectra of argon and nitrogen matrices, suggests that product B exists in three different matrix sites in solid argon. For the species isolated in site 1, absorbing at 844.7 and 879.5 cm^{-1} , the appearance of two triplets of bands in experiments with scrambled $^{16}\text{O}_{3-x}\text{O}_x$ indicates that B contains two equivalent oxygen atoms. The frequencies of these absorptions favor assignment to the symmetric and antisymmetric XO_2 (X = halogen) stretching modes respectively of IO_2 rather than ClO_2 . Furthermore, neither band exhibits a chlorine isotope shift expected for a chloryl species; the corresponding modes in chloryl fluoride, FCIO_2 , are shifted by -7.4 and -12.4 cm^{-1} , respectively, on substitution of ^{35}Cl by ^{37}Cl .¹⁸ The marked asymmetry of the two triplets is often observed in the spectra of dioxo species, for example, molybdenum dioxide¹⁹ and dioxochromium dicarbonyl, $(\text{OC})_2\text{CrO}_2$.²⁰ The greater separation between the symmetric and antisymmetric IO_2 stretching modes in $\text{I}^{16}\text{O}^{18}\text{O}$ (55.7 cm^{-1}) compared with I^{16}O_2 (34.8 cm^{-1}) or I^{18}O_2 (35.8 cm^{-1}) may be attributed to mixing between the two vibrations in the asymmetric isotope as a result of the decrease in symmetry. Assignment of the absorption at 879.5 cm^{-1} to the antisymmetric IO_2 stretch and that at 844.7 cm^{-1} to the symmetric IO_2 stretch is supported by both their relative intensity and the values of the ratios $\nu_{\text{sym}}(\text{I}^{16}\text{O}_2)/\nu_{\text{sym}}(\text{I}^{18}\text{O}_2)$ and $\nu_{\text{asym}}(\text{I}^{16}\text{O}_2)/\nu_{\text{asym}}(\text{I}^{18}\text{O}_2)$. Thus the intensity of the antisymmetric mode is greater than that of the symmetric vibration while the isotopic frequency ratio is lower. In these respects product B parallels NO_2 ,²¹ SO_2 ,²² and FCIO_2 .¹⁸ The absorptions at 330.5 and 324.5 cm^{-1} (sites 1 and 2) and 333.4 and 327.5 cm^{-1} (site 3) associated with product B exhibit no ^{18}O shift, and their position suggests assignment to an I-Cl stretching mode. The 6-cm^{-1} separation between components of the doublets supports this assignment, being attributed to the presence of two chlorine isotopes. Product B is therefore identified as iodyl chloride, O_2ICl .

The minor photoproduct C responsible for the band near 749 cm^{-1} remains unidentified. The band was relatively broad, in no experiment did it appear more than weakly, and it proved impossible to determine convincingly the effects of ^{18}O enrichment. The position of the band argues that it originates in a Cl-O or I-O stretching vibration, but it does not correspond to any known oxo-chlorine or -iodine species.⁸

Comparison of Spectra. It is of interest to compare the vibrational spectra of iodosyl chloride, OICl, and iodyl chloride, O_2ICl , with those of other species believed to contain discrete IO and IO_2 groups. Vibrations involving the IO and IO_2 moieties in IOSO_3CF_3 and $\text{IO}_2\text{SO}_3\text{X}$ (X = F, CF_3) are summarized in

(18) Robiette, A. G.; Parent, C. R.; Gerry, M. C. L. *J. Mol. Spectrosc.* **1981**, *86*, 455.

(19) Hewett, W. D., Jr.; Newton, J. H.; Weltner, W., Jr. *J. Phys. Chem.* **1975**, *79*, 2640.

(20) Poliakoff, M.; Smith, K. P.; Turner, J. J.; Wilkinson, A. J. *J. Chem. Soc., Dalton Trans* **1982**, 651.

(21) Laane, J.; Ohlsen, J. R. *Prog. Inorg. Chem.* **1980**, *27*, 465.

(22) Allavena, M.; Rysnik, R.; White, D.; Calder, V.; Mann, D. E. *J. Chem. Phys.*, **1969**, *50*, 3399.

Table IV. The Calculated and Observed Vibrational Frequencies (in cm^{-1}), Force Constants (in $\text{mdyne } \text{\AA}^{-1}$), and Geometric Parameters for the IO_2 Group in Iodyl Chloride, O_2ICl

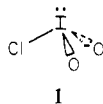
vib mode and force constant	$r_{10} = 1.625 \text{ \AA}, \alpha = 121^\circ$			observed frequencies		
	$^{16}\text{O}_2\text{ICl}$	$^{16}\text{O}^{18}\text{OICl}$	$^{18}\text{O}_2\text{ICl}$	$^{16}\text{O}_2\text{ICl}$	$^{16}\text{O}^{18}\text{OICl}$	$^{18}\text{O}_2\text{ICl}$
$\nu_{\text{asym}}(\text{IO}_2)$	879.5	868.2	837.4	879.5	868.6	837.4
$\nu_{\text{sym}}(\text{IO}_2)$	844.7	813.3	801.2	844.7	812.9	801.6
δIO_2	421.1	410.4	399.5	421	410.2	399.4
f_{10}		6.035				
$f_{10,10}$		-0.0828				
f_α		0.8044				
$f_{\alpha,10}$		-0.3873				

^aWith use of $r_{10} = 1.8 \text{ \AA}$, force constants are $f_{10} = 6.031$, $f_{10,10} = -0.0864$, $f_\alpha = 0.8055$, and $f_{\alpha,10} = -0.3928 \text{ mdyne } \text{\AA}^{-1}$. Calculated frequencies are identical except for δIO_2 which become 420.7 ($^{16}\text{O}_2\text{ICl}$), 410.0 ($^{16}\text{O}^{18}\text{OICl}$), and 399.1 cm^{-1} ($^{18}\text{O}_2\text{ICl}$).

Table III and compared with the vibrational frequencies observed for OICl and O_2ICl . The vibrational spectra of iodosyl and iodyl sulfonates^{9,12} have been interpreted in terms of discrete IO and IO_2 units. This may be contrasted with $(\text{IO})_2\text{SO}_4$ where the IO units are linked in infinite chains giving rise to infrared absorptions between 500 and 650 cm^{-1} .¹⁵ The close agreement between $\nu_{\text{sym}}(\text{IO}_2)$ and $\nu_{\text{asym}}(\text{IO}_2)$ for O_2ICl and $\text{O}_2\text{ISO}_3\text{X}$ ($\text{X} = \text{F}, \text{CF}_3$) supports the proposition of a discrete IO_2 group in $\text{O}_2\text{ISO}_3\text{X}$ since extended polymeric structures are most unlikely in argon matrices. On the other hand, the vibrational properties of OICl are less well matched by those of solid IOSO_3CF_3 .

Iodosyl chloride, $\text{O}=\text{I}-\text{Cl}$, should be an angular molecule with C_s symmetry. The measured $^{16}\text{O}/^{18}\text{O}$ and $^{35}\text{Cl}/^{37}\text{Cl}$ isotopic shifts imply that there is little coupling between the $\text{I}=\text{O}$ and $\text{I}-\text{Cl}$ stretching modes. In these circumstances and without any information about the third fundamental, the bending mode, we are not in a position to estimate the OICl bond angle from the vibrational frequencies of the different isotopes. The IO and ICl stretching force constants are about 5.0 and $1.7 \text{ mdyne } \text{\AA}^{-1}$, respectively; the corresponding parameters (in $\text{mdyn } \text{\AA}^{-1}$) for related species are as follows: IO 3.87 ,⁸ TeO (isoelectronic with IO^+) 5.33 ,²³ and ICl 2.39 .⁸ As with the comparison between ClO , $\text{O}=\text{Cl}-\text{Cl}$, and $\text{O}=\text{Cl}-\text{F}$ (with ClO force constants of 4.66 , 5.94 and $6.85 \text{ mdyne } \text{\AA}^{-1}$ respectively),^{5,24} these results imply that the ionic structure $\text{O}=\text{I}^+\text{Cl}^-$ makes a relatively large contribution to the bonding. Alternatively, the force constants may be said to signal the effective withdrawal of electron density from the IO ($p-p$) π^* orbitals through the interaction with the electronegative chlorine substituent.

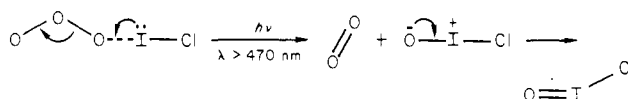
The similarity between the frequencies of the IO_2 stretching vibrations in O_2ICl and those of the analogous modes in tellurium dioxide, TeO_2 ,²⁵ also suggests a considerable degree of ionicity for the $\text{I}-\text{Cl}$ bond in iodyl chloride, since TeO_2 and IO_2^+ are isoelectronic. Iodyl chloride is expected to have a pyramidal structure (**1**), and ionic character in the $\text{I}-\text{Cl}$ bond should lead

**1**

to relatively little coupling between vibrational modes localized in the IO_2 unit and other modes. The relatively massive iodine atom should also minimize the mechanical coupling between the motions of the oxygen and chlorine atoms. In these circumstances it is profitable to perform normal coordinate calculations treating the IO_2 unit as a C_{2v} triatomic molecule in order to gain further support for the vibrational assignments and an estimate of the IO_2 bond angle.

The isotopic ν_3 frequency ratio leads to a $120 \pm 10^\circ$ estimate for the OIO bond angle with use of the relationships reported earlier.^{17,22} The antisymmetric stretching symmetry coordinate

Scheme I



force constant $F_{33} = f_{10} - f_{10,10} = 6.12 \text{ mdyne } \text{\AA}^{-1}$ was determined. The totally symmetric modes $\nu_{\text{sym}}(\text{IO}_2)$ and $\delta(\text{IO}_2)$ were calculated by using values of 1.625 and 1.80 \AA for the $\text{I}-\text{O}$ bond length, as observed in $p\text{-ClC}_6\text{H}_4\text{IO}_2$ and IO , respectively.⁸ The band observed at 421 cm^{-1} was assigned to δIO_2 on the basis of its shift to 399.4 cm^{-1} in $^{18}\text{O}_2\text{ICl}$ and the assignment of a band at 428 cm^{-1} to the same vibrational mode in $\text{O}_2\text{ISO}_3\text{F}$.⁹ Calculations for $^{16}\text{O}_2\text{ICl}$, $^{18}\text{O}_2\text{ICl}$, and $^{16}\text{O}^{18}\text{OICl}$ are summarized in Table IV; the success in reproducing nine vibrational frequencies within experimental error suggests that the IO_2 group in O_2ICl is indeed vibrationally independent of the chlorine atom and that the OIO angle is approximately 120° . This is reasonable in view of the $110 \pm 2^\circ$ calculated bond angle for matrix-isolated TeO_2 .²⁵

Ozone Complex. New bands at 1110.8 , 1019.5 , 372.1 , and 364.1 cm^{-1} in the ozone and iodine monochloride samples suggest a specific interaction between matrix-isolated O_3 and ICl molecules. As such, the absorbing species may be represented as $(\text{O}_3)_x \cdot (\text{ICl})_y$. The data in Figure 3 show that the concentration of $(\text{O}_3)_x \cdot (\text{ICl})_y$ is directly proportional to the concentration of O_3 present in the matrix and therefore $x = 1$. Under the present conditions, no direct measurement of y was possible although a very low concentration of ICl aggregate, as observed in nitrogen matrices, had no effect on the concentration of $(\text{O}_3)_x \cdot (\text{ICl})_y$. Thus these additional absorptions seem to be a product of monomolecular iodine monochloride, and it is proposed that $y = 1$ also.

Iodosyl and iodyl chloride are formed in these experiments under conditions in which isolated ozone cannot be photolyzed. Any oxygen atom transfer in this system is therefore a consequence of the photolysis ($\lambda > 470 \text{ nm}$) of the $\text{O}_3 \cdot \text{ICl}$ complex. Since the main products contain $\text{I}-\text{O}$ but not $\text{Cl}-\text{O}$ bonds, it appears that ozone is bound to ICl in the complex via the iodine atom. The infrared spectrum of the complex exhibits a displacement of the $\text{I}-\text{Cl}$ stretching vibration to lower frequency and an increased separation of the symmetric and antisymmetric stretching vibrations of ozone. A decrease in the $\text{I}-\text{Cl}$ mode can be explained by electron donation into the σ^* orbital of ICl . The perturbations observed for ozone most likely result from reduction in the symmetry of O_3 , which suggests a $\text{O}-\text{O}-\text{O}-\text{I}-\text{Cl}$ structure for the complex.

The complex $\text{O}_3 \cdot \text{ICl}$ absorbs near 460 nm and irradiation into this band leads to photolysis of the complex. The transition is interpreted in terms of charge transfer from ICl to O_3 in a manner similar to that proposed for π complexes between ozone and substituted benzenes.¹ It is perhaps noteworthy that the ICl submolecule in the $\text{O}_3 \cdot \text{ICl}$ complex absorbs at slightly longer wavelength than ICl itself, but it is the complex and not isolated O_3 and ICl that produces OICl on photolysis. The transformation of the complex to OICl is represented in Scheme I. The iodine atom is oxidized from the $+1$ to $+3$ oxidation state and oxygen is transferred to it, leaving dioxygen as the second product. The

(23) Huber, K. P.; Herzberg, G. "Molecular Spectra and Molecular Structure. IV. Constants of Diatomic Molecules"; Van Nostrand-Reinhold Co.: New York, 1979.

(24) Chi, F. K.; Andrews, L. *J. Phys. Chem.* **1973**, *77*, 3062.

(25) Spoliti, M.; Grosso, V.; Cesaro, S. N. *J. Mol. Struct.* **1974**, *21*, 7.

iodosyl chloride so formed is likely to be in an electronically or vibrationally excited state.

Mechanism of Iodyl Chloride Formation. Since irradiation of matrices containing scrambled $^{16}\text{O}_{3-x}^{18}\text{O}_x$ or $^{16}\text{O}_3$ and $^{18}\text{O}_3$ in the ratio 1:1 both yielded O_2ICl with a random distribution of oxygen isotopes, the two oxygen atoms in O_2ICl originate in different $\text{O}_3\cdot\text{ICl}$ complex molecules. The relative yield of O_2ICl and OICl increases in favor of the dioxo species as the photolysis temperature is increased which, together with the isotope data, implies that the formation of O_2ICl is diffusion controlled. It is proposed that electronically or vibrationally excited OICl formed during photolysis of $\text{O}_3\cdot\text{ICl}$ is either quenched, forming the observed iodosyl chloride product, or decomposes releasing an oxygen atom for reaction with another OICl to give O_2ICl .

Conclusions

Codeposition of ozone and iodine monochloride in argon, krypton, and nitrogen matrices leads to the formation of a specific molecular complex, $\text{O}_3\cdot\text{ICl}$. The complex photodissociates to iodosyl chloride OICl with visible light. The OICl photoproduct is probably formed initially in a vibrationally or electronically excited state and is either quenched by the matrix or dissociates to ICl and atomic oxygen. The release and diffusion of oxygen

atoms leads to formation of a second product iodyl chloride O_2ICl . Iodyl chloride becomes the favored product as the photolysis temperature is increased as a result of either a greater extent of diffusion of oxygen atoms through the matrix or a reduced efficiency in the quenching of excited iodosyl chloride.

This paper represents the first characterization of a monomolecular inorganic iodosyl compound. Normal coordinate analysis calculations applied to iodyl chloride treated the IO_2 moiety as vibrationally independent of the chlorine atom: frequencies for $\nu_{\text{sym}}(\text{IO}_2)$, $\nu_{\text{asym}}(\text{IO}_2)$, and $\delta(\text{IO}_2)$ for three isotopes $^{16}\text{O}_2\text{ICl}$, $^{18}\text{O}_2\text{ICl}$, and $^{16}\text{O}^{18}\text{OICl}$ could be fitted within experimental error. This implies little mechanical or electronic influence of the chlorine atom on the vibrations of the IO_2 moiety as a result of the large mass of iodine and substantial ionic character in the I-Cl bond. Polarity in the I-Cl bond is supported by the low frequency of the I-Cl stretching mode compared with iodine monochloride and the high frequency of the symmetric and antisymmetric stretching vibrations of the IO_2 group.

Acknowledgement is made to the donors of the Petroleum Research Fund, administered by the American Chemical Society, for support of this research and to the Science Research Council (U.K.) for a research studentship (D.J.D.).

Study of Disaccharide Conformation by Measurements of Nuclear Overhauser Enhancement, Relaxation Rates, and ^{13}C - ^1H Coupling: 1,6-Anhydro- β -cellobiose Hexaacetate

Photis Dais,* Tony K. M. Shing, and Arthur S. Perlin

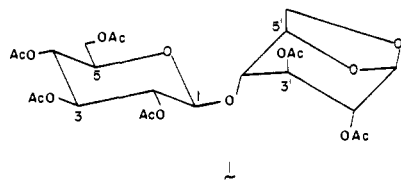
Contribution from the Department of Chemistry, McGill University, Montreal, Quebec H3C 3G1, Canada. Received June 9, 1983

Abstract: Nonselective and mono- and biselective spin-lattice relaxation rates, nuclear Overhauser enhancements, and coupling constants were measured as means for determining such stereochemical features as the conformation of the glucosidic bond of 2,3,4,6,2',3'-hexa-*O*-acetyl-4-*O*- β -D-glucopyranosyl-1',6'-anhydro- β -D-glucopyranose (**1**) in acetone- d_6 solution. Interproton distances within each ring of **1**, as well as of **2**, specifically C-deuterated samples of **1**, calculated from either a combination of monoselective relaxation rates and NOE experiments or mono- and biselective relaxation rates, agreed within ± 0.2 Å of those found in the crystal. However, substantially different values were obtained from nonselective relaxation rate measurements. The orientation of the glucosidic bond, as deduced from interresidue spin-spin coupling (3J) between the C-1,H-4' and C-4',H-1 nuclei, is described by dihedral angles ψ of 45-50° and ϕ of 25-30°. These values are within the region of the allowed conformation as defined by the interatomic distances H-1-H-4' and H-1-H-5' obtained from relaxation, NOE data, and by computer simulation.

The conformational properties of disaccharides have received a great deal of attention in recent decades, stimulated primarily by interest in the conformations of structurally related polysaccharides. There are various theoretical treatments of the subject,^{1,2} and several experimental techniques have been employed to determine disaccharide conformations in the solid state³⁻⁵ and in solution.⁶⁻¹⁰

One approach for examining conformation in solution is offered by proton monoselective spin-lattice relaxation experiments in combination with NOE data,^{11,12} and/or mono- and biselective

experiments¹³ that determine the magnitude of specific dipolar interproton spin-lattice relaxation contributions. This approach has been utilized in the present study for the quantitative measurement of interproton distances within disaccharide derivative **1**, i.e., 2,3,4,6,2',3'-hexa-*O*-acetyl-4-*O*- β -D-glucopyranosyl-1',6'-anhydro- β -D-glucopyranose (1,6-anhydro- β -cellobiose), in order to determine its conformation in solution. Compound **1** attracted



our interest because it introduces a marked departure in stereochemistry from other derivatives of cellobiose examined previously.^{9,10} Among other differences, the reducing end moiety of **1** possesses the opposite ($^1\text{C}_4$) chair conformation, and its (1 \rightarrow 4') linkage entails an axial, rather than equatorial, *O*-4'-. In earlier

- (1) Rees, D. A.; Skerrett, R. J. *Carbohydr. Res.* **1968**, *7*, 334.
- (2) Rees, D. A.; Smith, P. J. C. *J. Chem. Soc., Perkin Trans.* **1975**, *2*, 836.
- (3) Quigley, G. J.; Sarko, A.; Marchessault, R. H. *J. Am. Chem. Soc.* **1970**, *92*, 5834.
- (4) Ham, J. T.; Williams, D. G. *Acta Crystallogr., Sect. B* **1970**, *26*, 1373.
- (5) Chu, S. S. C.; Jeffrey, G. A. *Acta Crystallogr., Sect. B* **1968**, *24*, 830.
- (6) Casu, B.; Reggiani, M.; Gallo, G. G.; Vigevani, A. *Tetrahedron* **1966**, *22*, 3061.
- (7) Rees, D. A. *J. Chem. Soc., B* **1970**, 877.
- (8) Perlin, A. S.; Cyr, N.; Ritchie, R. G. S.; Parfondry, A. *Carbohydr. Res.* **1974**, *37*, C1.
- (9) Parfondry, A.; Cyr, N.; Perlin, A. S. *Carbohydr. Res.* **1977**, *59*, 299.
- (10) Hamer, G. K.; Balza, F.; Cyr, N.; Perlin, A. S. *Can. J. Chem.* **1978**, *56*, 3109.
- (11) Hall, L. D.; Wong, K. F. *J. Chem. Soc., Chem. Commun.* **1979**, 951.

- (12) Hall, L. D.; Hill, H. D. W. *J. Am. Chem. Soc.* **1976**, *98*, 1269.
- (13) Kaplan, D.; Navon, G. *J. Chem. Soc., Perkin Trans.* **2** **1981**, 1374.